Identification, Hysteresis, and Discrimination in Enzyme Kinetic Models

ROBERT D. TANNER

Merck & Co., Inc., Rahway, New Jersey 07065

Three kinetic rate constants and an initial enzyme concentration are estimated in Britton Chance's classical peroxidase model by applying both the Picard iteration-orthogonal polynomial and stationary state methods to his transient experimental data. Since this model does not describe the hysteresis exhibited by the data, more complex models are examined in order to account for this behavior. From a study of this hysteresis phenomena which is inherent to the structure of consecutive reactions, it is found that in addition to discriminating between mechanisms much useful information about the history of enzyme induction can be observed from the direction, shape, and area of the hysteresis loop.

Most enzyme kinetic experiments reported in the literature comprise measurements of either the substrate or the product initial rates of the reaction at varying initial substrate concentrations. These measurements are used to approximate the concentrations at the time of the stationary state, where the enzyme-substrate concentration is at a maximum. This approximation is indeed valid when the molar ratio of initial substrate to initial enzyme concentration is large. With such information, two composite parameters can be extracted from the Briggs-Haldane stationary state relationship fit to the data.

While the initial rate approach to enzyme kinetics is experimentally attractive, it is unsatisfactory for at least three reasons. First, the validity of the original dynamic mass action model cannot be tested directly without evaluating all of the individual rate constants and the initial enzyme concentration, which is typically unknown. Second, it is often desirable to know initial enzyme concentrations in moles per liter, rather than the arbitrary activity units of a lumped parameter. Absolute values of specific blood plasma enzyme concentrations would be useful, for example, in determining dosage levels of enzymatically degraded drugs. Knowledge of the time histories of induced enzyme concentrations could, moreover, lead to dynamic therapeutic drug administration strategies. And third, as pointed out by Garfinkel et al. (5), there is evidence that within some living cells enzyme concentrations exceed substrate concentrations, so that kinetic responses from these systems could not be meaningfully analyzed with a Briggs-Haldane (or the historical antecedent, Michaelis-Menten) type of equation.

In order to obtain more complete enzyme kinetic information, therefore, we simultaneously measure two or more concentration-time trajectories, generally the substrate and product concentrations. Such information, however, is often difficult to obtain. An ultraviolet spectrometer, for example, usually can measure only one of the chemical species without interference in the linear Beer's law concentration domain, although multiple wavelength readings can obviate this problem when interpreted by a nonlinear analysis. Another difficulty, in practice, is that the initial transients of enzyme reactions take place in millisecond or even microsecond time periods and cannot be observed with standard laboratory equipment. While the stopped-flow or the temperature jump relaxation apparatus can measure these rapid changes, such methods have not been widely adopted. It is felt, however, that the additional difficulty required to obtain such information is more than compensated for by its usefulness in elucidating the mechanism of enzymatic reactions.

In this paper we shall therefore examine stopped-flow enzyme kinetic data, choosing for an example the classical peroxidase reaction measurements and model developed by Chance (2). We deliberately omit using Chance's equilibrium data, as a departure from Chance's early analysis, to see if kinetic data alone can supply sufficient information for identifying the parameters in the model.

While the truncated polynomial analysis of the initial transient proposed by Gutfreund and Roughton (4) is attractive as a means for extracting rate constants in this problem, it is not at all clear as to how restrictive this truncation process is in practice. We propose, therefore, to fit the initial data in the same spirit with polynomials but not restrict ourselves to either the linear or quadratic term. In so doing we will not obtain unique solutions of the parameters but rather bounds which are functions of the fitting polynomial degree. These bounds in turn roughly reflect the variability of the data.

Consequently, the coupling of the initial transient data analysis with a conventional stationary state approach provides the means for obtaining four algebraic relationships to solve for the three unknown rate constants and the initial enzyme concentration in this model. Since any approximate parameter estimation technique can be refined by a gradient least-squares parameter search, we could improve these parameter estimates if desired. Conversely, gradient search techniques are complemented by the approximate estimation scheme developed here because the complexity of the hill climbing methods requires fairly accurate priming values to initiate the proper direction for the climb and hence insure convergence.

What is perhaps most interesting about Chance's data is not that it can be used to test various parameter estimation schemes, but rather that a hysteresis curve results when the product rate is graphed as a function of the enzyme-substrate complex. We have already observed such behavior in fermentation systems, and have used it to conclude that a reaction step was enzymatically catalyzed (6). While the connection between these two different systems is not obvious, it is shown that the hysteresis results be-

cause both reactions are comprised of sequential steps. Series or consecutive reactions, in general, exhibit hysteresis when a product rate is plotted against a generated precursor which does not directly precede the irreversibly formed product. The direction and shape of this hysteresis loop is especially useful in elucidating enzyme concentration histories and discriminating between postulated models.

CHANCE'S MODEL AND DATA

Britton Chance proposed in 1943 that the following chemical mechanism described his stopped-flow measurements of the peroxidase reaction system (2):

$$S_1 + E \underset{k_2}{\overset{k_1}{\rightleftarrows}} ES$$

$$ES + S_2 \xrightarrow{k_3} P + E,$$

where

S_1	=	hydrogen peroxide
E	=	horseradish peroxidase enzyme
ES	=	enzyme-substrate complex
S_2	=	leucomalachite green $= A\,H_2$
P	=	malachite green $= A$
k_i	=	rate constant i

His work was the first to directly compare transient enzyme kinetic data with a computer simulation of the enzyme-substrate mathematical model. This was offered as evidence for the validity of the Michaelis-Menten model, as modified by Briggs and Haldane, which is central to exploring the behavior of enzymes. Chance's direct measurement of the ES complex laid to rest any lingering doubts about its existence and important role in enzyme mechanisms.

We shall now estimate the parameters in the model using a new, computationally simple, parameter estimation scheme (7) and compare the values we obtain with Chance's more precise estimates. Even though Chance knew the starting concentration of enzyme, it will be considered here as a parameter to be estimated—the more typical situation in enzyme kinetics. Moreover, we shall not include the equilibrium data for the first reaction in order to see if the kinetic data alone are sufficient to estimate all of the parameters. The graphical data analyzed and exhibited in Figures 1 and 2 were taken at 25°C. and a pH of 4. The trajectories on these figures were simulated by Chance on an analog computer for the following rate constants and initial concentrations:

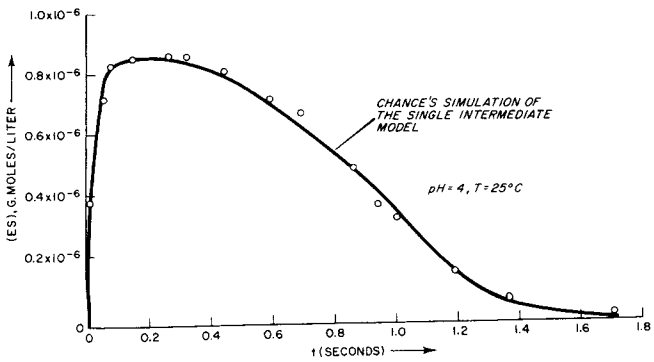

Fig. 1. Horseradish peroxidase-hydrogen peroxide formation. B. Chance's classified experimental data (1943).

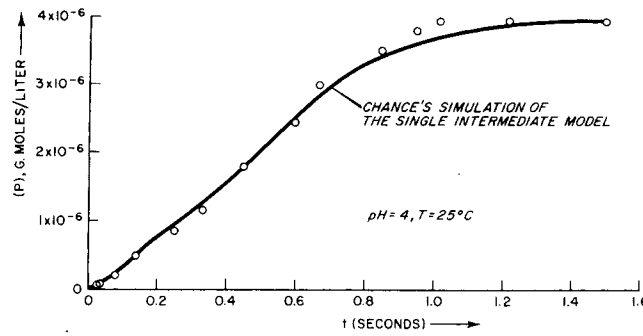

Fig. 2. Malachite green formation in the horseradish peroxidase catalyzed hydrogen peroxide-leucomalachite green reaction. B. Chance's classical experimental data (1943).

k_1	=	0.9×10^7 liters/(mole)(sec.)
k_2	=	0
k_3	=	3×10^5 liters/(mole)(sec.)
$(S_1)_0$	=	4×10^{-6} moles/liter
$(S_2)_0$	=	15×10^{-6} moles/liter
$(E)_0$	=	1×10^{-6} moles/liter
$(ES)_0$	=	0
$(P)_0$	=	0

The differential equations developed to describe the single intermediate model using the law of mass action are

$$\frac{d(S_1)}{dt} = -k_1\,(S_1)\,(E) + k_2\,(ES); \quad (S_1)_0 = S_1^* \tag{1}$$

$$\frac{d(S_2)}{dt} = -k_3\,(ES)\,(S_2); \quad (S_2)_0 = S_2^* \tag{2}$$

$$\frac{d(E)}{dt} = -k_1\,(S_1)\,(E) + k_2\,(ES) + k_3\,(ES)\,(S_2);$$

$$(E)_0 = E^* \tag{3}$$

$$\frac{d(ES)}{dt} = k_1\,(S_1)\,(E) - k_2\,(ES) - k_3\,(ES)\,(S_2);$$

$$(ES)_0 = 0 \tag{4}$$

$$\frac{d(P)}{dt} = k_3\,(ES)\,(S_2); \quad (P)_0 = 0 \tag{5}$$

where the time t is in seconds.

These equations in turn imply three algebraic constraints between the variables

$$(S_1) + (P) - (E) = S_1^* - E^* \tag{6}$$

$$(E) + (ES) = E^* \tag{7}$$

$$(P) + (S_2) = S_2^*. \tag{8}$$

There are therefore two degrees of freedom for this model comprised of five variables and three constraints. In other words, the above model is completely defined when the time trajectories of the two concentration variables ES and P are measured. It is fortunate that ES is one of the measured species here, rather than S, because when ES is computed from 6 and 7 using S and P it could become the small difference between two nearly equal numbers and, hence, contain large numerical errors.

PARAMETER ESTIMATION

Our strategy for estimating k_1, k_2, k_3, and E^* from the kinetic data is to first obtain two algebraic relationships

of these parameters from data including the initial transient region ($0 \leq t \leq 0.08$ sec.), using the orthogonal polynomial-Picard iteration method. Then we shall apply the stationary state assumption over the remaining time trajectory to derive a two substrate extension of the Michaelis-Menten equation, and, thereby, obtain two more algebraic relationships. These four equations are then solved to give the desired four parameters. We note that the stationary state assumption is valid when S_1^*/E^* is "large" (*1*). Here, the value of four for S_1^*/E^* appears to be adequately large to meet this condition, albeit marginally. We also observe that we could have applied the orthogonal polynomial-Picard iteration method directly to the stationary state domain, and would have done so had S_1^*/E^* been small. That approach was avoided here, however, because it leads to more complex (and nearly singular) algebraic relationships than the stationary state equations (*7*).

Applying Picard's iteration method to the system of Equations (1) to (5), we obtain the following polynomials for ES and P in the time domain $0 \leq t \leq T$

$$(ES) = (k_1 S_1^* E^*)t + \text{higher degree terms in } t,$$

and

$$(P) = \left\{ \frac{k_1 k_3 S_1^* E^*}{2} \right\} t^2 + \text{higher degree terms}$$

Curve fitting the data with the least-squares orthogonal polynomials of degrees m and m', respectively:

$$(ES) = at + bt^2 + ct^3 + \ldots.$$

and,

$$(P) = a't^2 + b't^3 + c't^4 + \ldots,$$

gives us numerical values for a and a' as functions of m, m' and T. Equating the corresponding first coefficients in the orthogonal polynomials with those in the Picard polynomials results in the desired two relationships, which in the limit as $T \to 0$ and m and $m' \to \infty$ are exact for continuous, error-free data:

$$\lim_{\substack{T \to 0 \\ m \to \infty}} a(m, T) = k_1 S_1^* E^*$$

and

$$\lim_{\substack{T \to 0 \\ m' \to \infty}} a'(m', T) = \frac{k_1 k_3 S_1^* S_2^* E^*}{2}.$$

Estimates for a and a' for the discrete experimental data are obtained by extrapolating T to 0 in Figures 3 and 4 for the low integer sequence of polynomial degrees, m and m' to give (*7*):

$$a(m) = \lim_{T \to 0} a\,(m, T) \simeq k_1 S_1^* E^* \qquad (9)$$

and

$$a'(m') = \lim_{T \to 0} a'\,(m', T) \simeq \frac{k_1 k_3 S_1^* S_2^* E^*}{2} \qquad (10)$$

The starred values in these figures are the numbers computed for a and a' from Equations (9) and (10) with Chance's estimated rate constants and known initial enzyme concentration.

The fitting domain for a is restricted to $T = 0.08$ sec. in order to avoid bending the ES least-squares polynomial about the stationary-point in Figure 1. By restricting T in this way, we can insure that the ES polynomial is reasonably accurate for low polynomial degrees. Since the data for P in Figure 2 are ordered in in a monotonically increasing progression, we can accurately fit $a'(m')$ over the entire time trajectory, a much larger T than that used to obtain a. This results in maximizing the information

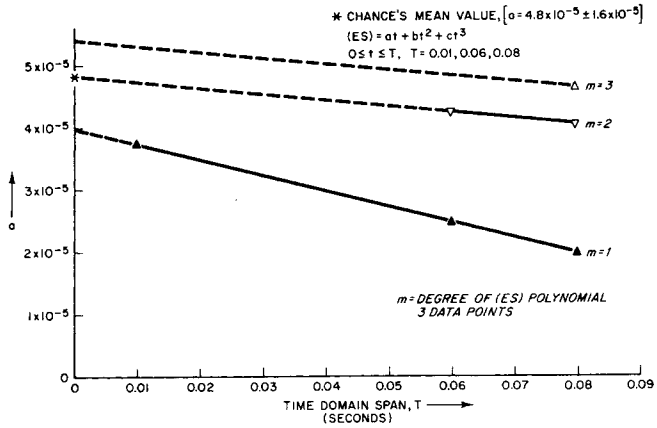

Fig. 3. First *(ES)* coefficient versus initial fitted time domain span, with the degree of the orthogonal least squares polynomial as a parameter. B. Chance's classical peroxidase reaction data (1943).

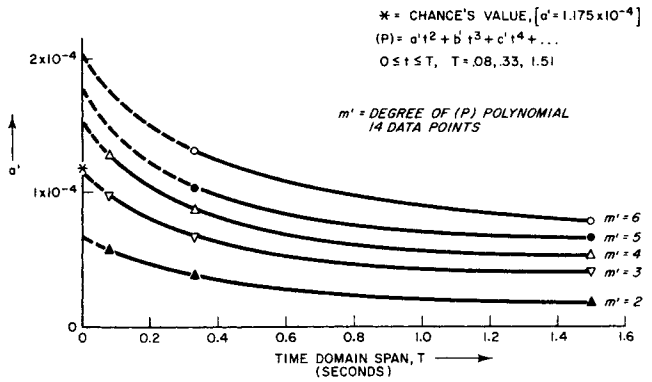

Fig. 4. First *(P)* coefficient versus fitted time domain span, with the degree of the orthogonal least squares polynomial as a parameter. B. Chance's classical peroxidase reaction data (1943).

available, as reflected by the greater number of polynomial degrees for a' than a. On the other hand, the large domain seems to introduce spurious resolution of the data, as evidenced by the significant deviation of $a'(m')$, for large m', from Chance's a'. We observe from Figure 3 that all of the $a(m)$ values lie within Chance's variance for a, that is, $a = 4.8 \times 10^{-5} \pm 1.6 \times 10^{-5}$, so that any $a(m)$ could be considered as a good estimate.

The stationary-state relationship for Chance's model is obtained by setting $d(ES)/dt = 0$ in Equation (4) and then solving for (ES) using Equation (7). Substituting this expression for (ES) into (5) gives the desired result

$$\frac{d(P)}{dt} = \frac{k_3 E^*\ (S_1)(S_2)}{(S_1) + \dfrac{k_2 + k_3\,(S_2)}{k_1}}$$

As $k_3(S_2)$ approaches a constant (for example, when S_2 is very large as in the case of water), the above expression reduces to the familiar Briggs-Haldane single substrate equation. In order to extract the lumped parameters in this equation from a two dimensional graph, we rearrange the equation to the form

$$\frac{(S_1)\ (S_2)}{\dfrac{d(P)}{dt}} - \frac{(S_2)}{k_1 E^*} = \frac{1}{k_3 E^*}\left[\ (S_1) + \frac{k_2}{k_1}\ \right]$$

Since we don't know $k_1 E^*$ at this point we substitute

Equation (9) into this formula and, at the same time, effectively smooth the (P) differences by employing Equations (5) and (10) to obtain:

$$\frac{(S_1)\ S_2^*\ a(m)}{2(ES)\ a'(m')} - \frac{(S_2)\ S_1^*}{a(m)} = \frac{1}{k_3 E^*}\left[(S_1) + \frac{k_2}{k_1}\right] \tag{11}$$

Plotting the left side of Equation (11) versus S_1 in moles/liter, where $(S_1) = S_1^* - (P) - (ES)$, and $(S_2) = S_2^* - (P)$ gives the two composite parameters describing the stationary state domain

$$\frac{1}{k_3 E^*} = \text{slope} \tag{12}$$

$$\frac{k_2}{k_1 k_3 E^*} = \text{intercept} \tag{13}$$

Typical graphs of (11) for several m and m' combinations are shown in Figure 5. The fact that the data are reasonably ordered by straight lines tends to verify the stationary state assumption. It is observed that all but one of these lines has a negative intercept, implying a nonrealistic negative parameter. Since k_3 can be evaluated from the ratio of Equation (10) to (9), E^* from (12), and k_1 from (9), so that all three of these parameters are computed to be positive, it follows that when k_2 is calculated from (13) using these three computed values and the nonpositive intercept, it too will be nonpositive. The negative values for k_2, however, just reflect the small variance near the value of zero:

$$k_2 = (\text{intercept})\ (k_1 k_3 E^*) = (\text{intercept})\left[\frac{2a'}{S_1^*\ S_2^*}\right].$$

The largest negative value for k_2 is therefore

$$k_2\ (m = 1,\ m' = 6) \simeq -2/(15)\ (\text{sec.})$$

This small value for k_2 compares favorably with Chance's estimate, $k_2 \leq 1.33 \times 10^4$, obtained from equilibrium measurements. Chance's number is essentially zero (1/1000) with respect to k_1, which is 10^7. Chance, in fact, used the value of zero in simulating his model.

Since the slope of these lines is $1/k_3 E^*$, we can compute E^* from

$$E^*\ (m, m') = \frac{S_2^*\ a(m)}{(\text{Slope})\ 2a'(m')} \tag{14}$$

over the stationary state domain. Because we don't know how to choose m and m' a priori in practice, it is most fortunate that the estimated values for E^* are nearly independent of m and m' when computed from Equation (14)

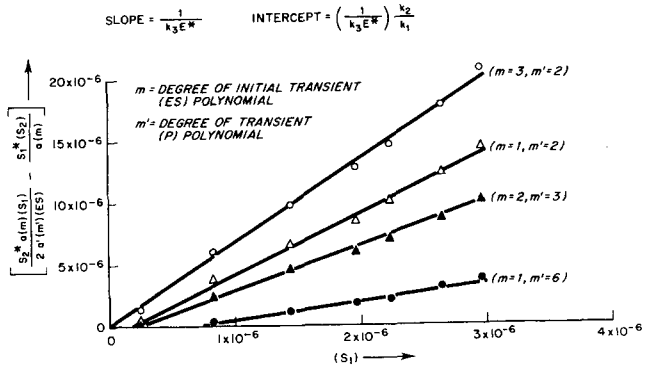

Fig. 5. Stationary state data for selected transient polynomial degrees. B. Chance's classical peroxidase reaction data (1943)—single enzyme-substrate intermediate model.

$$0.86 \times 10^{-6} \leq E^*\ (m, m') \leq 0.982 \times 10^{-6}$$

The reason that m and m' nearly cancel out of the computation (1×10^{-6} is the known value for E^*) is now explained. We do this by deriving an analytical expression for E^* using the same procedure followed in calculating $E^*\ (m, m')$ above.

We first assume that the following relationships hold in the stationary state domain (they are, in fact, consistent with the data)

$$d\left[\frac{(S_1)}{(ES)}\right] \Big/ d\ (S_1) = \frac{k_3}{k_1}\frac{1}{(E)} \simeq \alpha, \tag{15}$$

where α = constant

$$\frac{d(S_2)}{d(S_1)} = 1 \tag{16}$$

and

$$\frac{S_1^*}{a(m)} << \frac{S_2^*\ a(m)\alpha}{2a'(m')} \tag{17}$$

Equations (15) and (16) are restatements of the stationary state assumption, with the additional assumption that α is constant. Equation (17) reduces to $(ES) >> 0$, an inequality in keeping with the data in Figure 1 over the stationary state domain.

Differentiating (11) with respect to (S_1) and invoking (15), (16), and (17) leads to the desired relationship

$$E^*(\alpha) \simeq \frac{1}{\alpha} = \frac{d\ (S_1)}{d\left[\frac{(S_1)}{(ES)}\right]} \tag{18}$$

The parameter α is obtained directly from the slope of the line $(S_1)/(ES)$ plotted versus (S_1) so that for these data

$$\frac{1}{\alpha} = 0.826 \times 10^{-6}$$

a value close to the known value for E^*. We have shown, therefore, that $E^*(\alpha) \approx E^*\ (m, m')$, so that when we are given transient data for ES and S_1, E^* can be computed directly from (18) when $\alpha \approx$ constant. Equation (18) incidentally has also been used to estimate E^* within 10% of its known value, given three place accuracy data simulated from a single enzyme, single substrate model, where $k_i = 1$ $(i = 1, 2, 3)$, $E^* = 0.1$, and $S^* = 1$. What is most attractive about the ease with which we estimate E^*, using (14) or (18), is that it is feasible to estimate unknown enzyme concentrations in absolute units (grams moles/liter) rather than in one of the various arbitrary activity units. The formula in (18) may be restricted to data which include the direct measurement of ES. This is because at least three place data are required to accurately compute ES from the difference between used substrate and formed product.

Now that we have estimated E^* between 0.82×10^{-6} and 0.98×10^{-6}, we shall now proceed to numerically evaluate the three rate constants. From (9) and (10)

$$k_3 = \frac{2\ a'(m')}{S_2^*\ a(m)}$$

Therefore

$$1.65 \times 10^5 \leq k_3\ (m, m') \leq 6.87 \times 10^5,$$

which reflects the moderate variance associated with the larger m' values of $a'(m')$, when compared with Chance's more refined bounds for k_3 of

$$2.8 \times 10^5 \leq k_3 \leq 3.46 \times 10^5$$

As previously noted, we will call $k_2 \approx 0$. Finally, since from (9)

$$k_1 = \frac{a(m)}{S_1^* E^* (m, m')}$$

it follows that

$$1.02 \times 10^7 \leq k_1 (m, m') \leq 1.65 \times 10^7,$$

bounds which nearly match Chance's values

$$k_1 = (1.2 \pm 0.4) \times 10^7$$

With the possible exception of the computed k_3, therefore, all of these estimated values agree quite well with Chance's estimates for his original model. Moreover, averages of the smallest and largest parameter estimates give quite respectable estimates when compared with Chance's values. Another applicable averaging technique would be to average $a(m)$ and $a'(m')$ before computing the parameters.

The variances of these estimated parameters could be tightened somewhat by iterating with a second-order gradient least-squares parameter search, a procedure which would most likely converge to a "nearby" local optimum using the above estimates for the starting vector. But since Chance has already refined these parameters adequately, as noted by the satisfactory match between his simulated model and the data in Figures 1 and 2, it is unnecessary for us to do so. What is more important is to see where the original model does not adequately describe the data, and then, if necessary, develop alternate models to overcome the deficiencies. We restrict ourselves to the original data in this analysis, although it is recognized that measurements of several other intermediate states have been made since this early study (3).

If Equation (5) adequately describes the data, then a plot of $d(P)/dt$ versus (ES) (S_2) is a straight line. We notice, however, that when smoothed $\Delta P/\Delta t$ is plotted against ES $[S_2^* - (P)]$, or for that matter ES, a hysteresis curve results, as shown in Figure 6. Chance's original model is, therefore, inadequate for characterizing these data as acknowledged by Chance in his later work (3). We shall endeavor, therefore, to account for this hysteresis with one of Chance's more complex models. As background for this development, we will first examine simpler cases of hysteresis arising in consecutive chemical reactions.

HYSTERESIS IN CONSECUTIVE REACTIONS

We shall now develop the mathematical basis for the memory phenomena of chemical reactions in series. This development will also apply to other systems in series, such as radioactive decay or photochemical reactions. Here we shall first analyze linear (first-order) systems, and then examine the structure of the more complex enzymatic reactions. In the next section we will use this analysis for discriminating between candidate models describing the peroxidase catalyzed reaction.

For the four species chemical network:

$$A \xrightarrow{k_1} B \xrightarrow{k_2} C \xrightarrow{k_3} D,$$

we observe in Figure 7 that when B is generated as the reaction proceeds, a counterclockwise hysteresis trajectory develops. The relationship describing the hysteresis loop in Figure 7 derived from the linear differential equation model is

$$\frac{d(D)}{dt} = k_2(B) - \frac{d(C)}{dt} = k_2(B) - \frac{1}{k_3}\frac{d^2(D)}{dt^2} \qquad (19)$$

Since $d(C)/dt$ is initially positive, because C is generated internally, and negative finally, $d(D)/dt$ will be less than $k_2(B)$ at first and greater at the end. The greatest value of B is at the point where $d(B)/dt = 0$, prior to the junction of the upper and lower branches, on the line $k_2(B)$, where $d(C)/dt = 0$. We can, therefore, evaluate k_2 directly from the maximum $d(D)/dt$ point. The area circumscribed by the hysteresis curve collapses to zero when k_3 becomes very large, that is, when $(C) \rightarrow 0$. Another interesting observation is that if a feedback loop from D to B is introduced with a rate constant k_4 we obtain

$$\frac{d(D)}{dt} = k_2(B) - \left[k_4(D) + \frac{d(C)}{dt} \right] \qquad (20)$$

For pronounced feedback, it is conceivable for $k_4(D)$ to eventually become larger in absolute value than $d(C)/dt$, resulting in a reversal of direction, or a clockwise hysteresis function. Consequently, the direction of the loop is useful for determining whether a feedback path is significant in the reaction.

It is even easier to conceive of the hysteresis resulting from the modified experiment where A is completely reacted, stopping at B, followed by B reacting to D via C. In this case, the time trajectory follows the shape of a loop like that in Figure 9. For the limiting case, when k_3 becomes very large, that is $(C) \rightarrow 0$, a discontinuity results. This loop is the perimeter of the triangle shown on Figure 7.

The more biologically relevant model, comprised of series enzymatic reactions, also exhibits hysteresis. We shall illustrate one type of hysteresis with the two enzyme-two substrate model:

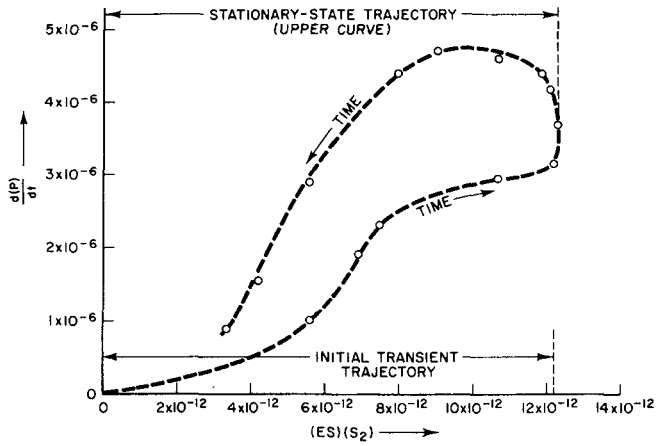

Fig. 6. Rate of malachite green formation as a function of (ES) (S_2). B. Chance's classical peroxidase reaction data (1943).

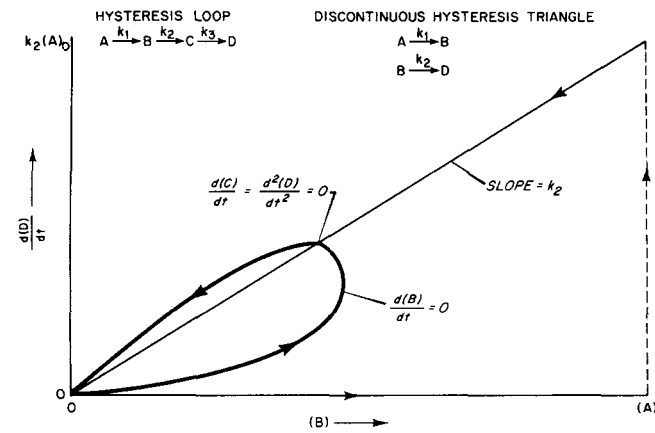

Fig. 7. Two hysteresis paths for a series chemical network.

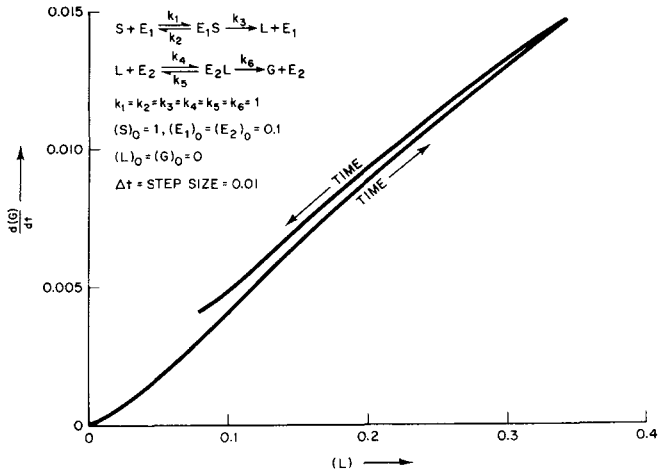

Fig. 8. Computer simulation of a sequential double enzyme system.

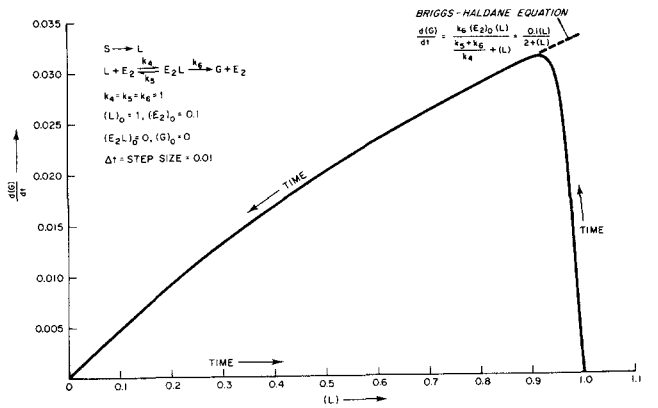

Fig. 9. Computer simulation of the sequential double enzmye system broken into two steps.

$$S + E_1 \underset{k_2}{\overset{k_1}{\rightleftarrows}} E_1S \xrightarrow{k_3} L + E_1$$

$$L + E_2 \underset{k_5}{\overset{k_4}{\rightleftarrows}} E_2L \xrightarrow{k_6} G + E_2,$$

by relating $d(G)/dt$ to (L). Since the system of nonlinear differential equations describing this model, based on the law of mass action, does not reduce to a simple and general relationship between $d(G)/dt$ and (L) over the entire time trajectory, we shall look at digitally simulated results. For the model $k_i = 1$ for all i, and $S^* = 1$, $L^* = 0$, $G^* = 0$, and $E_1^* = E_2^* = 0.1$, we produce, for a time step size of 0.01 and a total time of 90 arbitrary units, the graph in Figure 8.

The question now arises whether the gap between the forward and reverse arcs in Figure 8 could be observed experimentally, since at the widest separation the difference is about 10%. Perturbing the rate constants does not widen this separation. For example, increasing k_4 rotates the entire function counterclockwise and increasing k_3 lengthens or stretches the function. In both perturbations, the widest difference between the arcs remains around 10%.

We do observe, however, that if E_2 is introduced as a function of time, we can separate these curves significantly. In doing so, this closed system becomes open with respect to enzyme addition. We are already familiar with the two step process where E_2 is a step function. This is essentially the route followed when we start with $S^* = 1$ and form all L, given $E_2 = 0$. (This step could be as simple as reaching for reagent L on the laboratory shelf, knowing that L came from S.) Then continuing from $L^* = 1$ and introducing $E_2^* = 0.1$, we obtain the familiar hyperbola (7), with a tail, of the form in Figure 9.

If E_2 is added from outside the reaction broth according to the proportional feedforward relationship

$$\left.\frac{d(E_2)}{dt}\right|_{\text{added}} = K(S)$$

then we simulate a curve with the shape of Figure 10. What is so interesting about such aging behavior is that it is very similar to that already observed in data describing the gluconic acid fermentation system (6), as shown in Figure 11. In this system

S = glucose
L = gluconolactone
G = gluconic acid
E_1 = glucose dehydrogenase
and E_2 = lactonase.

The lactonase addition (actually generated within the system at the expense of glucose) term in Figure 11 is, of

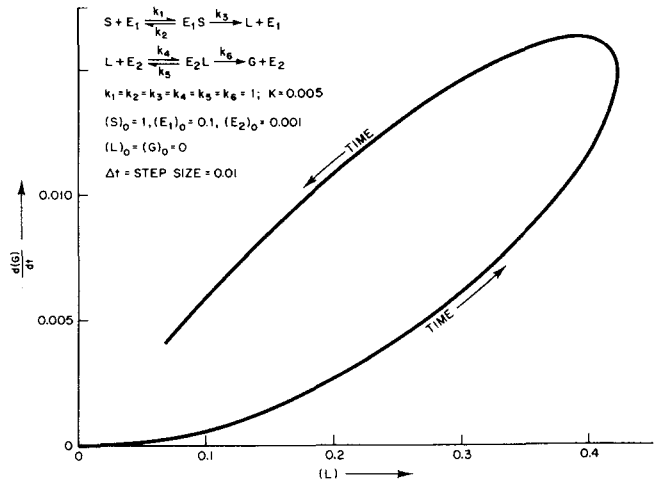

Fig. 10. Computer simulation of a sequential double enzyme system with programmed addition of the second enzyme.

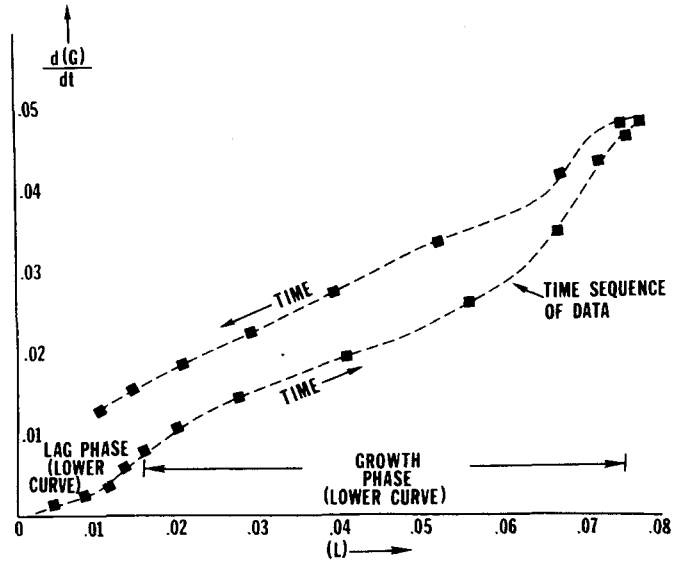

Fig. 11. Hysteresis function describing product formation rate in the gluconic acid fermentation.

course, only approximated by $K(S)$. It is more likely that it is proportional to the polysomal concentration in the cell and only indirectly proportional to the precursor substrate (6). Nevertheless, the hysteresis behavior shown in Figure 11 is qualitatively simulated by the construct illustrated in Figure 10 assuming that the contributions of other metabolic pathways such as glycolysis and gluconeogenesis are negligible. We note that inclusion of nonenzymatic hydrolysis in the model, that is, $L \rightarrow G$, merely rotates the curve in Figure 11 and does not distort the shape of the hysteresis loop.

What we have demonstrated, therefore, is that analysis of the hysteresis curve can serve as a vehicle for studying the enzyme generation term. In other words, attributing the divergence, shape, and area of the hysteresis curve to an enzyme generation term is a way for interpreting and continuously monitoring the induction of an enzyme. Since the area circumscribed by a magnetic hysteresis curve is used as a measure of the "losses" or inefficiencies of that system, we may, similarly, use this reaction hysteresis area as a measure of the efficiency of product yield. Figure 8, representing a continuous catalytic conversion, then describes a nearly 100% efficient system while Figure 9 depicts the corresponding process decomposed to two separate steps as being only a few percent efficient.

DISCRIMINATION BETWEEN ENZYMATIC MODELS

Now that we have developed some experience with the hysteresis property of series reactions, we shall formulate a model whose structure qualitatively exhibits the behavior observed in Figure 6. To do this, we first see if Chance's updated peroxidase model (3, 4) comprised of two enzyme-substrate complexes and one free radical (for a two hydrogen donating second substrate), can account for this effect. His updated model is expressed by the scheme

$$E + S_1 \underset{k_2}{\overset{k_1}{\rightleftarrows}} ES_I$$

$$ES_I + S_2 \xrightarrow{k_3} ES_{II} + AH^{\bullet}$$

$$ES_{II} + S_2 \xrightarrow{k_4} E + AH^{\bullet}$$

$$2AH^{\bullet} \xrightarrow{k_5} P + S_2,$$

where the two additional variables are

$AH^{\bullet}$ = a free radical intermediate

and

ES_{II} = measured ES

Four of the seven differential equations describing this model are

$$\frac{d(ES_{II})}{dt} = k_3\,(ES_I)\,(S_2) - k_4\,(ES_{II})\,(S_2); \quad (ES_{II})_0 = 0 \qquad (21)$$

$$\frac{d(AH^{\bullet})}{dt} = k_3\,(ES_I)\,(S_2) + k_4\,(ES_{II})\,(S_2) - k_5\,(AH^{\bullet})^2; \quad (AH^{\bullet})_0 = 0 \qquad (22)$$

$$\frac{d(S_2)}{dt} = -k_3\,(ES_I)\,(S_2) - k_4\,(ES_{II})\,(S_2) + \tfrac{1}{2}\,k_5\,(AH^{\bullet})^2; \quad (S_2)_0 = S_2^{*} \qquad (23)$$

$$\frac{d(P)}{dt} = \tfrac{1}{2}\,k_5\,(AH^{\bullet})^2; \quad (P)_0 = 0 \qquad (24)$$

From the differential equations, three constraining algebraic relationships are obtained, so it follows that there are four degrees of freedom for this model. With only two chemical species measured, we will not attempt to evaluate all of the rate constants explicitly, since there is not enough information. What we will be concerned with is whether $d(P)/dt$ plotted against (ES_{II}) (S_2) gives a counterclockwise hysteresis curve. In this way we can discriminate between the earlier single enzyme-substrate intermediate model and more complex models.

From Equations (21), (23), and (24) we obtain

$$\frac{d(P)}{dt} = 2k_4\,(ES_{II})\,(S_2) + \frac{d(S_2)}{dt} + \frac{d(ES_{II})}{dt} \qquad (25)$$

Since from the data

$$\left|\frac{d(ES_{II})}{dt}\right| > \left|\frac{d(S_2)}{dt}\right| \qquad (26)$$

a plot of $d(P)/dt$ against (ES_{II}) (S_2) gives a clockwise hysteresis curve. This follows because ES_{II}, as an intermediate, is generated initially and then used up as the reaction proceeds in time. We could describe this clockwise hysteresis effect with a simpler relationship if we make the reasonable assumption that

$$\frac{d(S_2)}{dt} \simeq -\frac{d(P)}{dt} \qquad (27)$$

another way of saying $d(AH^{\bullet})/dt \simeq 0$. In this approximate case Equation (25) becomes

$$\frac{d(P)}{dt} \simeq k_4\,(ES_{II})\,(S_2) + \tfrac{1}{2}\,\frac{d(ES_{II})}{dt} \qquad (28)$$

Since the data exhibited in Figure 6 show hysteresis in the opposite direction, we reject this two enzyme-substrate, single free radical model as a candidate for representing the data, given the measured $ES = ES_{II}$. We also note that when S_2 is computed with Equation (8), a relationship predicated on the validity of Chance's original model, rather than the constraint obtained from summing (22) to (24), we make the reasonable assumption that $(AH^{\bullet})$ is negligible with respect to (S_2).

We could still use the model, however, if the measured $ES = ES_I$. This follows because

$$\frac{d(P)}{dt} = 2k_3\,(ES_I)\,(S_2) + \frac{d(S_2)}{dt} - \frac{d(ES_{II})}{dt} \qquad (29)$$

or assuming $d(AH^{\bullet})/dt = 0$ as before, we obtain

$$\frac{d(P)}{dt} = k_3\,(ES_I)\,(S_2) - \tfrac{1}{2}\,\frac{d(ES_{II})}{dt} \qquad (30)$$

Therefore, as demonstrated by (29) or (30), the model exhibits counterclockwise hysteresis, in agreement with the data plotted in Figure 6, if the measured $ES = ES_I$.

One way that we can reconcile the claim, that the measured ES is the second enzyme-substrate complex with the counterclockwise hysteresis effect in the above model, is to add the additional rearrangement step, $ES_I \underset{k_4}{\overset{k_3}{\rightleftarrows}} ES_{II}$, to Chance's updated model, and postulate the modified model

$$E + S_1 \underset{k_2}{\overset{k_1}{\rightleftarrows}} ES_I$$

$$ES_I \underset{k_4}{\overset{k_3}{\rightleftarrows}} ES_{II}$$

$$ES_{II} + S_2 \xrightarrow{k_5} ES_{III} + AH^{\cdot}$$

$$ES_{III} + S_2 \xrightarrow{k_6} E + AH^{\cdot}$$

$$2AH^{\cdot} \xrightarrow{k_7} P + S_2 \quad .$$

The analogous equation to (30) for the modified model then becomes

$$\frac{d(P)}{dt} = k_5 (ES_{II}) (S_2) - \tfrac{1}{2} \frac{d(ES_{III})}{dt} \qquad (31)$$

an equation which describes the counterclockwise hysteresis effect, given the measured $ES = ES_{II}$. As a final thought, we observe from Equation (31) that k_5 can be evaluated from the point at which $d(ES)_{III}/dt = 0$. We assume that this point is also close to the largest abscissa point on the curve in Figure 6, where $d(ES_{II})/dt = 0$, so that

$$k_5 \approx \frac{4 \times 10^{-6}}{12 \times 10^{-12}} = 1/3 \times 10^6 \text{ liters/(mole)(sec.)},$$

a value in close agreement with the k_3 describing the ES and S_2 addition step in Chance's original model.

It is now appropriate to discuss the effect of cumulative errors, inherent to the smoothed values of $\Delta P/\Delta t$, on the discrimination between competing models. We shall not give a detailed analysis of the experimental errors, but demonstrate that the probability of a change in direction in the hysteresis curve occurring by chance is rather remote. We restrict this argument to three possible configurations describing the data depicted in Figure 6: a straight line and both clockwise and counterclockwise hysteresis curves.

The probability of any given point being independently located at random above or below a straight line through the origin on such a plot is ½. Therefore, the probability of all of the points being randomly ordered in a particular arrangement about a ray from the origin through the point demarking the transient and stationary-state zones is of the order of $(\tfrac{1}{2})^{n-1}$, a miniscule number when $n = 14$ total points. Because the points are ordered in time (counterclockwise) even when the differences are unsmoothed, the configuration in Figure 6 shall be called nonrandom and, hence, not a straight line.

To further differentiate between a clockwise and counterclockwise curvature direction, we now determine the probability of the lower arc being transposed above the upper arc (the most likely rearrangement which could cause hysteresis direction reversal). Reasoning as above, the probability of this event occurring is of the order of $(\tfrac{1}{2})^5$ or about 3% of the time, still an improbable random experiment. We, therefore, feel confident that the points graphed in Figure 6 are in fact ordered in a counterclockwise fashion.

CONCLUSIONS

The rate constants and initial enzyme concentration in the single enzyme-substrate peroxidase reaction model were easily estimated to values within the precision of the data, using the Picard iteration-orthogonal polynomial and stationary state techniques. While identifying these parameters, a new stationary state relationship was developed for computing the initial enzyme concentration, independent of the other system constants. It therefore seems feasible to employ kinetic data as an analytical tool for determining concentrations of enzymes in solution.

In order to understand the hysteresis behavior of the product rate function, a study was made of this memory property which is inherent to consecutive reactions. From this analysis, the efficiency of the reaction steps, connecting intermediate components to products, was categorized according to the area circumscribed by the hysteresis loop. The contours of this loop, moreover, were shown to be useful in elucidating the time course of enzyme induction and in discriminating between competing models.

NOTATION

a = first coefficient in (ES) orthogonal polynomial
a' = first coefficient in (P) orthogonal polynomial
A, B, C, D = chemical species in a series chemical network
$AH^{\cdot}$ = free radical
E = enzyme
ES = enzyme-substrate complex
G = gluconic acid
K = $d(E_2)/dt/(S)$, where (E_2) is the added enzyme
k_i = rate constant i
L = gluconolactone
m = degree of (ES) orthogonal polynomial
m' = degree of (P) orthogonal polynomial
P = product
S = substrate
t = time
T = fitting time domain for the orthogonal polynomial

Greek Letters

α = $d\left[\frac{(S_1)}{(ES)}\right] \Big/ d(S_1)$
Δ = difference operator applied to time or concentration

Subscripts

0 = time zero
1, 2 = substrate, enzyme, or rate constant index
I, II, III = enzyme-substrate complex index

Superscripts

° = initial concentration
′ = coefficient or degree marker for the (P) orthogonal polynomial

LITERATURE CITED

1. Aris, R., "Chemical Kinetics and the Ecology of Mathematics," *Am. Scien.*, **58**, 419-428 (1970).
2. Chance, B., "The Kinetics of the Enzyme—Substrate Compound of Peroxidase," *J. Biol. Chem.*, **151**, 553-577 (1943).
3. Chance, B., "The Kinetics and Stoichiometry of the Transition from the Primary to the Secondary Peroxidase Peroxide Complexes," *Arch. Biochem. and Biophys.*, **41**, 416-424 (1952).
4. Dixon, M., and E. C. Webb, "Enzymes," Second Edit., Academic Press Inc., 102-111, 311-313, New York (1964).
5. Garfinkel, D., L. Garfinkel, M. Pring, S. B. Green, and B. Chance, *Annual Review Of Biochemistry*, **39**, 490, Annual Reviews, Inc., Palo Alto (1970).
6. Tanner, R. D., "An Enzyme Kinetc Model for Describing Fermentation Processes," *Biotechnology and Bioengineering*, **12**, 831-843 (1970).
7. Tanner, R., "Estimating Kinetic Rate Constants Using Orthogonal Polynomials and Picard's Iteration Method," *Ind. Eng. Chem. Fundamentals*, **11**, 1 (1972).

Manuscript received June 22, 1971; revision received November 9, 1971; paper accepted November 10, 1971.